

## 8B.1 SPACED-ANTENNA INTERFEROMETRY TO DETECT DISCRETE OBJECTS AND SUB-VOLUME INHOMOGENEITIES OF REFLECTIVITY

Guifu Zhang<sup>1\*</sup>, Richard J. Doviak<sup>2</sup>, and Xuetao Chen<sup>1</sup>

1: University of Oklahoma, Norman, OK 73072

2: National Severe Storms Laboratory, Norman, OK 73072

### 1. INTRODUCTION

Weather radar theory is commonly based on an assumption of wave scattering in a statistically homogenous medium (Doviak and Zrnic, 2006). Often this is not valid because the radar resolution volume  $V_6$  can be large at far ranges and inhomogeneities are likely to exist within  $V_6$ . For example, the beam width of the WSR-88D, is about 1 km at a range of 60 km and it is likely that reflectivity gradients exist across  $V_6$ . For example, a brightband/melting layer has thickness less than 0.5km. Non-uniform beam filling can bias radar measurements of reflectivity and cause error in rain estimation, also noted that the inhomogeneity within a radar beam causes error in wind measurement (Cohn et al., 2001). Recent study shows the effects of incomplete beam-filling on polarimetric radar observables (Ryzhkov, 2007). Oversampling and data assimilation techniques are being used to obtain detailed information within the beam (Xue et al, 2006, Yu et al. 2006; Zhang et al, 2005).

A Spaced-Antenna Interferometer (SAI) can measure wind, shear and turbulence, within  $V_6$ . A SAI also has potential to detect and locate discrete objects and sub-volume reflectivity inhomogeneities within  $V_6$ . The National Weather Center's (NWC) phased-array weather radar, called the National Weather Radar Testbed (NWRT) located in Norman, Oklahoma offers such opportunities to advance weather radar techniques. Zhang and Doviak (2007) examined the capabilities of SAI to measure crossbeam wind using the NWRT. Transverse shear of the radial component of wind and anisotropic turbulence were taken into account, but the reflectivity field was assumed to be homogenous.

In this study, we consider the spatial inhomogeneity of reflectivity field and its effects on radar measurements. SAI theory is extended to detect and locate discrete objects and sub-volume reflectivity inhomogeneities. Auto- and cross-correlation functions are derived based on wave scattering by a large object and clusters of randomly distributed particles. The antenna separation, mean wind, shear and anisotropic turbulence are all taken into account in the formulation. This paper is organized as follows: Section 2 describes the effect of sub-volume inhomogeneity on radar measurements and the principle of SAI for the detection of inhomogeneities. SAI theory is based on wave scattering from randomly distributed scatterers in Section 3; Section 4 discusses the detection of a large object and the inhomogeneities of randomly distributed scatterers using the NWRT as a SAI.

### 2. CONCEPTUAL DESCRIPTION OF SAI TO DETECT SUB-VOLUME INHOMOGENEITIES

Weather radar detects echoes from point scatterers and random fluctuation of refraction index. The 'point' scatterers can be large objects (e.g., birds, aircraft, etc.), or randomly distributed small particles such as hydrometeors.

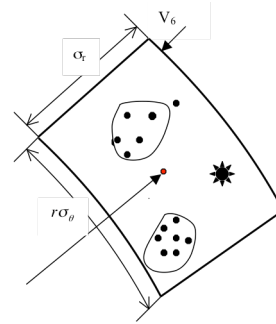


Figure 1: Sketch of hydrometeor density inhomogeneities, and a single large discrete object (star) in  $V_6$ .

As sketched in Fig. 1, there is a large object and two clusters of hydrometeors in  $V_6$ . The inhomogeneities affect the assignment of locations to the measured reflectivity and Doppler velocity. Furthermore, it is difficult to precisely locate the object, detect the existence of the sub-volume inhomogeneities, and quantify the strength of the inhomogeneities using common weather radars. The measurements of reflectivity, radial wind and spectrum width are not sufficient to separate an individual object from distributed scatterers.

The NWRT uses an antenna from the AN/SPY1-A radar of the Navy's Aegis system. The antenna provides sum, azimuth difference, and elevation difference signals. The sum and difference signals can be processed to effectively retrieve the signals from the left and right, and upper and lower, halves of the antenna, thus forming a SAI (Fig. 2). The phase center for the transmitting antenna (also that for receive sum) is indicated by "T", and that for two receiving antennas from each half are denoted as "R<sub>1</sub>" and "R<sub>2</sub>" respectively. Other effective phase centers can be formed by auto/cross-correlation processing. An object or a cluster of hydrometeors at different locations in the volume, have different relative phases with respect to the antenna phase centers, thus allowing its location to be determined.

The principle of SAI for detecting sub-volume inhomogeneity can also be understood through an effective beam width. Having a non-uniform reflectivity field across the beam is equivalent to having a narrower transmitting beam, or a larger

\* Corresponding author: Guifu Zhang, School of Meteorology, University of Oklahoma, Norman, OK 73072  
Email: guzhang1@ou.edu

transmitting antenna. Thus the correlation length (characteristic scale) of interference pattern on the antenna plane increases, and hence the cross-correlation coefficient at zero lag will increase. This will affect the performance of SAI for cross beam wind measurement because SAI relies on a broad angular distribution of scatterers. Nevertheless, the SAI can still detect the object and/or reflectivity inhomogeneity as shown in next section.

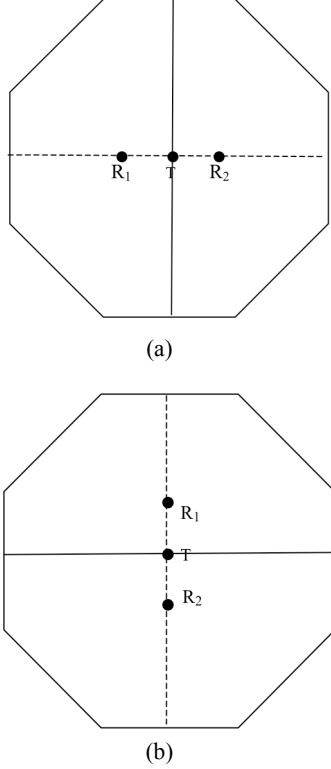


Figure 2: Location of SAI phase centers. The transmitting and receiving phase centers are marked with solid dots. The separation of the receiving phase centers is about 1.22 meters calculated from antenna pattern measurements for the NWRT.

### 3. FORMULATION FOR SAI IN THE PRESENCE OF SUB-VOLUME INHOMOGENEITY

Following Zhang and Doviak (2007), we have a received signal at  $R_1$  expressed by the sum of that caused by each scatterers as follows

$$V(\vec{r}_{01}, t_1) = A_{10}W_{10} \exp[-jk(l\vec{r}_0 - \vec{r}_1(t_1)l + l\vec{r}_{01} - \vec{r}_1(t_1)l)] + \sum_{n=1}^N A_{1n}W_{1n} \exp[-jk(l\vec{r}_0 - \vec{r}_n(t_1)l + l\vec{r}_{01} - \vec{r}_n(t_1)l)] \quad (1)$$

where the first term is the echo from the discrete object and the summation is the echo from all the randomly distributed hydrometeors.  $A_{10}$  is the prefilter scattering amplitude from the object, and  $A_{1n}$  is the prefilter scattering amplitude from the  $n$ th scatterer located at  $\vec{r}_n(t_1)$  at time  $t_1$ ,  $\vec{r}_{01}$  is the vector distance from the center of  $V_6$  to the receiver at  $R_1$ , and  $W_{10}$  and  $W_{1n}$  are range dependent weights, a function of the

transmitted pulse width and the receiver filter's bandwidth, as well as the range location of the object and the  $n$ th hydrometeor within  $V_6$ . Because the range extent of  $V_6$  is usually small compare to  $r_0$  the small changes in the weighting function  $W(r)$  due to the  $1/r_0^2$  factor can be ignored. The angular and range weighting functions are expressed as

$$A_i(\vec{r}(t)) = A_0 g_T^{1/2} g_R^{1/2} \exp \left[ -\frac{z'^2(t)}{4r_0^2 \sigma_{\theta T}^2} - \frac{(z'(t) - z'_i)^2}{4r_0^2 \sigma_{\theta R}^2} - \frac{y'^2(t)}{4r_0^2 \sigma_{\phi T}^2} - \frac{(y'(t) - y'_i)^2}{4r_0^2 \sigma_{\phi R}^2} \right] \quad (2a)$$

$$W_i(\vec{r}(t)) = \exp \left[ -\frac{x'^2(t)}{4\sigma_R^2} \right], \quad (2b)$$

where:  $i = 1, 2$  and  $(y'_i, z'_i)$  are the locations of the SA receivers,  $\sigma_R^2$  is the second central moment of the range weighting function assumed equal for both receivers,  $\sigma_{\theta T}$  and  $\sigma_{\theta R}$  are the square roots of the second central moment of the one-way power weighting functions along the zenith for the transmitting and receiving antennas respectively,  $\sigma_{\phi T}$  and  $\sigma_{\phi R}$  are, correspondingly, those beamwidths along the azimuth.

A similar expression to (1) can be obtained for the received signal at  $R_2$ . Thus the cross-correlation of signals from the two receivers can be written as

$$C_{12}(t_1, t_2) = \langle V^*(\vec{r}_{01}, t_1) V(\vec{r}_{02}, t_2) \rangle. \quad (3)$$

To include the reflectivity inhomogeneity, we model the number density  $n_l(\vec{r})$  with a set of clusters represented by

$$n(\vec{r}) = \sum_{l=1}^M n_l \exp \left[ -\frac{(x' - x'_l)^2}{2L_{lx'}^2} - \frac{(y' - y'_l)^2}{2L_{ly'}^2} - \frac{(z' - z'_l)^2}{2L_{lz'}^2} \right] \quad (4)$$

where  $n_l$  is the maximal number density of the  $l$ th inhomogeneous cell;  $L_{lx'}$ ,  $L_{ly'}$ , and  $L_{lz'}$  are the characteristic sizes in the  $x'$ ,  $y'$ , and  $z'$  direction, respectively.

We consider that turbulence and shear are also present in the volume. For narrow beams, motion  $v_{x'}$  parallel to the beam axis causes most phase shifts and signal fluctuation.

Therefore. We assume  $v_{x'}$  can be expressed as the Taylor series to first order in  $\vec{r}$ ,

$$v_{x'}(\vec{r}) = v_{x'}(0) + v_{lx'} + s_{x'}x' + s_{y'}y' + s_{z'}z', \quad (5)$$

where  $v_{x'}(0)$  is the mean wind component at the center of  $V_6$  and parallel to the beam axis,  $v_{lx'}$  is the corresponding turbulent component, and  $\vec{s} = \nabla v_{x'}(\vec{r})$  is the shear assumed uniform across  $V_6$ . Further, turbulence  $v_{lx'}$  is assumed to be statistically homogeneous, having a Gaussian probability distribution with a zero mean and a standard deviation  $\sigma_{lx'}$ .

Following the procedure in Zhang and Doviak (2007), we derive the cross-correlation function. Substituting (1) into (3), using (2), (4) and (5), and performing integrations, we obtain

$$\begin{aligned}
C_{12}(t, \tau) = & |A_0|^2 g_T g_R \exp \left[ -\frac{z_0'^2}{2r_0^2 \sigma_{\theta T}^2} - \frac{y_0'^2}{2r_0^2 \sigma_{\theta R}^2} - \frac{z_0'^2 + \Delta z_{12}'^2 / 4}{2r_0^2 \sigma_{\theta R}^2} - \frac{y_0'^2 + \Delta y_{12}'^2 / 4}{2r_0^2 \sigma_{\theta R}^2} \right] \\
& \times \exp \left[ 2jk v_{Tx} \tau + 2jk \left( z_0' (v_{Oz} \tau - \Delta z_{12}' / 2) + y_0' (v_{Oy} \tau - \Delta y_{12}' / 2) \right) / r_0 \right] \\
& + |A_0|^2 g_T g_R 2^{1/2} \pi^{3/2} \sum_{l=1}^M n_l \sigma_{lR} r_0^2 \sigma_{l\theta} \sigma_{l\phi} \times \\
& \exp \left[ -\frac{x_l'^2}{2L_{lx'}^2} + 2jk v_{lx} (0) \tau + 2\sigma_{lR}^2 \left( jk s_{lx} \tau + \frac{x_l'}{2L_{lx'}} \right)^2 - 2k^2 \sigma_{lx}^2 \tau^2 \right] \\
& \exp \left[ -\frac{y_l'^2}{2L_{ly'}^2} + 2\sigma_{l\theta}^2 \left( jk (v_{cy}(0) \tau + r_0 s_{ly} \tau - \Delta y_{12}' / 2) + \frac{r_0 y_l'}{2L_{ly'}} \right)^2 - 2k^2 \sigma_{l\theta}^2 \sigma_{ly}^2 \tau^2 \right] \\
& \exp \left[ -\frac{z_l'^2}{2L_{lz'}^2} + 2\sigma_{l\phi}^2 \left( jk (v_{cz}(0) \tau + r_0 s_{lz} \tau - \Delta z_{12}' / 2) + \frac{r_0 z_l'}{2L_{lz'}} \right)^2 - 2k^2 \sigma_{l\phi}^2 \sigma_{lz}^2 \tau^2 \right] \quad (6)
\end{aligned}$$

with

$$\sigma_{lR} = \left( \frac{1}{L_{lx'}^2} + \frac{1 + (1 + s_{lx} \tau)^2}{2\sigma_R^2} \right)^{-1/2} \quad (7a)$$

$$\sigma_{l\theta} = \left( \frac{r_0^2}{L_{ly'}^2} + \frac{1}{\sigma_{\theta T}^2} + \frac{1}{\sigma_{\theta R}^2} \right)^{-1/2} \quad (7b)$$

and

$$\sigma_{l\phi} = \left( \frac{r_0^2}{L_{lz'}^2} + \frac{1}{\sigma_{\theta T}^2} + \frac{1}{\sigma_{\theta R}^2} \right)^{-1/2} \quad (7c)$$

The above derivation follows exactly that given by Zhang and Doviak (2007), except that we now include scatter from a single discrete object (the first term in (4)), and allow hydrometeors to bunched into ellipsoidal clusters. Note that approximations of  $s_{lx} \tau \ll 1$ , and  $\frac{v_{cx} + s_{ly} y' + s_{lz} z'}{4\sigma_R} \ll 1$  have been

used in deriving (6). Eqs. (6), (7) constitute a general formulation for the SAI to detect and locate a reflectivity inhomogeneity and/or discrete objects within  $V_6$ . Fourier transform of (6) yields the cross-spectrum power density which allows discrimination of the scattering centers if their velocities are not the same.

## 4. ANALYSIS OF THE CROSS CORRELATION

### 4.1 Discrete object detection and location

The first term in (6) is the correlation function for the discrete object moving with a constant velocity. Its detection is based upon its correlation time (i.e., spectrum width) and its location within  $V_6$  can be determined from the relative phase at zero time-lag. That is,

$$z_0' = -\frac{\angle C_{12\theta}(t, 0)}{k \Delta z_{12}'} r_0 \quad (8a)$$

and

$$y_0' = -\frac{\angle C_{12\phi}(t, 0)}{k \Delta y_{12}'} r_0 \quad (8b)$$

This can be complementary to the monopulse method for the target location.

### 4.2 Reflectivity inhomogeneity detection and location

Assume there is only one cluster of randomly distributed hydrometeors within the beam. When the characteristic scale of the cluster is much larger than radar resolution volume size, i.e.,  $L_{lx'} \gg \sigma_R$ ,  $L_{ly'} / r_0 \gg \sigma_{\theta T}$  and  $L_{lz'} / r_0 \gg \sigma_{\theta R}$ , the second term of (6) reduces to

$$\begin{aligned}
C_{12}^{(in)}(t, \tau) = & |A_0|^2 g_T g_R 2^{1/2} \pi^{3/2} n_l \sigma_R r_0^2 \sigma_{e\theta} \sigma_{e\phi} \times \\
& \exp \left[ 2jk v_{lx}(0) \tau - 2\sigma_R^2 (k s_{lx} \tau)^2 - 2k^2 \sigma_{lx}^2 \tau^2 \right] \\
& \exp \left[ -2k^2 \sigma_{e\phi}^2 (v_{cy}(0) \tau + r_0 s_{ly} \tau - \Delta y_{12}' / 2)^2 - 2k^2 \sigma_{e\phi}^2 \sigma_{ly}^2 \tau^2 \right] \\
& \exp \left[ -2k^2 \sigma_{e\theta}^2 (v_{cz}(0) \tau + r_0 s_{lz} \tau - \Delta z_{12}' / 2)^2 - 2k^2 \sigma_{e\theta}^2 \sigma_{lz}^2 \tau^2 \right] \quad (9)
\end{aligned}$$

$$\text{where } \sigma_{e\phi} = \left( \frac{1}{\sigma_{\theta T}^2} + \frac{1}{\sigma_{\theta R}^2} \right)^{-1/2} \quad (10a)$$

and

$$\sigma_{e\theta} = \left( \frac{1}{\sigma_{\theta T}^2} + \frac{1}{\sigma_{\theta R}^2} \right)^{-1/2} \quad (10b)$$

Eq. (9) is essentially the same as that for uniform reflectivity field developed in Zhang and Doviak (2007).

On the other hand, when the characteristic scale of the cluster is much smaller than radar resolution volume size, i.e.,  $L_{lx'} \ll \sigma_R$ ,  $L_{ly'} / r_0 \ll \sigma_{\theta T}$  and  $L_{lz'} / r_0 \ll \sigma_{\theta R}$ . In this case, we have

$$\begin{aligned}
C_{12}^{(in)}(t, \tau) = & |A_0|^2 g_T g_R 2^{1/2} \pi^{3/2} n_l L_{lx'} L_{ly'} L_{lz'} \times \\
& \exp \left[ -2jk v_{lx}(0) \tau - 2k^2 \sigma_{lx}^2 \tau^2 \right] \\
& \exp \left[ -\frac{y_l'^2}{2L_{ly'}^2} + 2 \left( jk L_{ly'} (v_{cy}(0) \tau + r_0 s_{ly} \tau - \Delta y_{12}' / 2) / r_0 + \frac{y_l'}{2L_{ly'}} \right)^2 - 2k^2 L_{ly'}^2 \sigma_{ly}^2 \tau^2 / r_0^2 \right] \\
& \exp \left[ -\frac{z_l'^2}{2L_{lz'}^2} + 2 \left( jk L_{lz'} (v_{cz}(0) \tau + r_0 s_{lz} \tau - \Delta z_{12}' / 2) / r_0 + \frac{z_l'}{2L_{lz'}} \right)^2 - 2k^2 L_{lz'}^2 \sigma_{lz}^2 \tau^2 / r_0^2 \right] \quad (11)
\end{aligned}$$

Furthermore, the zero-lag correlation function is

$$\begin{aligned}
C_{12}^{(in)}(t, 0) = & \frac{C_{12}^{(in)}(t, 0)}{S^{(in)}(t, 0)} \\
= & \exp \left[ -\frac{k^2 L_{ly'}^2 \Delta y_{12}'^2}{2r_0^2} - \frac{k^2 L_{lz'}^2 \Delta z_{12}'^2}{2r_0^2} - \frac{jky_l' \Delta y_{12}'}{r_0} - \frac{jkz_l' \Delta z_{12}'}{r_0} \right] \quad (12)
\end{aligned}$$

Since  $L_{ly'} / r_0 \ll \sigma_{e\phi}$ , the cross-correlation coefficient given by (11) is larger than that of (9). Hence, the cross-correlation magnitude can be used to detect the in-homogeneity of reflectivity field, while the phase may be used to locate the inhomogeneity within  $V_6$ .

## 5. SUMMARY AND CONCLUSIONS

We develop the SAI technique to detect and locate a discrete object and/or reflectivity inhomogeneity within a radar's resolution volume. We formulate the problem based on wave scattering by the object and clusters of random particles.

It is shown that correlation magnitudes can be used for detection while the phase of auto- and cross-correlation functions can be used to locate the object or reflectivity inhomogeneity. The SAI technique can be implemented jointly with spectrum analysis for further advancement.

## Acknowledgements

Many thanks go to Lockheed Martin and NSSL's engineers for developing the NWRT. This work was partially supported by NOAA/NSSL under the cooperative agreement NA17RJ1227.

## 6. REFERENCES

- Cohn, S. A., W. O. J. Brown, C. L. Martin, M. S. Susedik, G. Maclean, and D. B. Parsons, 2001: Clear Air Boundary Layer Spaced Antenna Wind Measurement with the Multiple Antenna Profiler (MAPR), *Annales Geophysicae*, **19**(8), 845-854.
- Doviak, R. J., and D. S. Zrnic, 2006: *Doppler radar and weather observations*. Dover Publications Inc., Mineola, New York, 562 pp.
- Doviak, R. J., R. J. Lataitis, and C. L. Holloway, 1996: Cross correlation and cross spectra for spaced antenna wind profilers: 1. Theoretical analysis. *Radio Sci.* **31**, 157-180.
- Hardwick, K. M., S. J. Frazier, A. L. Pazmany, 2005: Spaced antenna measurements of cross beam velocity in severe storms. *32nd Int. Conf. on Radar Meteorology*, Albuquerque, NM., Amer. Meteor. Soc, P4R.11.
- Ryzhkov, A. V., 2007: The Impact of Beam Broadening on the Quality of Radar Polarimetric Data, *J. Atmos. Ocean. Tech.*, **24** (5): 729-744.
- Xue, M., S. Liu, and T. Yu, 2006: Variational Analysis of Oversampled Dual-Doppler Radial Velocity Data and Application to the Analysis of Tornado Circulations, *J. Atmos. Ocean. Tech.*, **23** (2): 228-240.
- Yu, T., G. Zhang, A. B. Chalamalasetti, R. J. Doviak, and D. Zrnic, 2006: Resolution enhancement using range oversampling, *J. Atmos. Ocean. Tech.*, **23** (2): 228-240.
- Zhang, G., T. Yu, and R. J. Doviak, 2005: Angular and range interferometry to refine weather radar resolution, *Radio Science*, vol. 40, RS3013, doi:10.1029/2004RS003125.
- Zhang, G., and R. J. Doviak, 2007: Spaced-antenna interferometry to measure crossbeam wind, shear and turbulence: Theory and formulation, *J. Atmos. Ocean. Tech.* **24**(5), 791-805.